J. Geotech. Eng., JSCE, No. 750/III-65, 1-14, 2003 December

EXPERIMENTAL STUDY ON LOAD SUPPORT SYSTEMS OF RUBBLE ROCK FOUNDATIONS

Masafumi MIYATA[1], Takahiro SUGANO[2], Takashi NAGAO[3], Masami NAKAGAWA[4], Graham G.W. MUSTOE[5], Tsuyoshi TANAKA[6] and Nobuo KIKUCHI[7]

[1]Member of JSCE, M. Eng., Senior Researcher, Coastal Disaster Prevention Div., NILIM (National Institute for Land and Infrastructure Management) (Nagase 3-1-1, Yokosuka, Kanagawa 239-0826, Japan)
[2]Member of JSCE, Dr. Eng., Head, Structural Dynamics Div., Port and Airport Research Institute (Nagase 3-1-1, Yokosuka, Kanagawa 239-0826, Japan)
[3]Member of JSCE, Dr. Eng., Head, Coastal Disaster Prevention Div., NILIM
[4]Ph.D., Assoc. Professor, Mining Eng. Department, Colorado School of Mines (Golden, Colorado 80401, USA)
[5]Ph.D., Professor, Division of Engineering, Colorado School of Mines (Golden, Colorado 80401, USA)
[6]Member of JSCE, Japan Science and Technology Corp. (Honcho 4-1-8, Kawaguchi, Saitama 332-0012, Japan)
[7]Yokohama Research and Engineering Office for Port and Airport, Ministry of Land, Infrastructure and Transport (Hashimoto 2-1-4, Kanagawa-ku, Yokohama, Kanagawa 221-0053, Japan)

In this study, we conducted a series of loading tests to investigate load support systems of a rubble rock foundation supporting a breakwater caisson. The test results show that the loading block is supported by a small number of contact points and the contact forces have a wide range of distribution. This discrete and inhomogeneous load support system of the foundation is very different from linearly distributed load support system assumed in the current design. As a result, the bottom slab of a caisson has larger bending moments than those predicted by linearly distributed load. The test results do not show a dependence of the load support system on the foundation surface roughness made by expert divers.

Key Words : *rubble rock foundation, load support system, vertical loading test, surface roughness, bending moment*

1. INTRODUCTION

Most of the Japanese breakwaters are of a composite type with heavy caissons resting on rubble rock foundations as shown in **Figure 1**. In constructing the rubble rock foundation, expert divers rearrange rubble rocks and prepare a smooth contacting surface to avoid concentrated loads acting on the bottom slab of a caisson. We call such a surface a "smooth surface". On the other hand, a "rough surface" exists in the areas where a caisson does not rest on the rubble. In order to shorten construction periods and reduce the associated costs for the foundation, the Ministry of Land, Infrastructure and Transport (MLIT) of Japan is now proposing to employ a rougher surface instead of a "smooth surface". However, it is suspected that an increase of the surface roughness might increase bending moment on the bottom slab of a caisson because the bottom slab may be supported by a smaller number of contact points for a rougher surface foundation[1)]. However, to date there is no experimental data or information about how a caisson is actually supported by a rubble rock foundation even for the smooth surface. As to the effects of the surface roughness on the load support

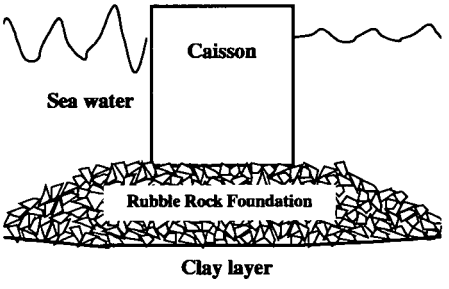

Fig.1 Cross section of a composite type breakwater

system of the rubble rock foundation, no comprehensive study exists.

In this study, we conducted a series of vertical loading tests using full-scale rubble rock foundations to investigate characteristics of load support systems of the foundation and the differences between the smooth and the rough surfaces made by expert divers. For this purpose, in the test we measured individual contact force between a rubble rock and the bottom of a loading block by using a unique measurement system. Since the test results showed discrete and inhomogenous load support systems, based on FEM analyses we also investigate how the inhomogenous load support system affects the bending moment amplitudes and spatial distributions of a square slab from the point of view of the difference in the design bending moment.

2. EXPERIMENTAL METHOD

(1) Experimental setup

Figure 2 shows a photograph of the loading test apparatus including rubble rocks, a loading block and two actuators to load the foundation beneath the block. Cross sectional and front views of the experimental apparatus are shown in **Figure 3**. The loading block is made of reinforced concrete whose height and widths are 1.0 m, 2.5 m and 2.5 m respectively. The block weight is about 180 kN.

In order to measure the contact forces between the rubble rocks and the loading block, we have developed a new measurement system. The system consists of 625 load gauges that are installed on the whole areas of the bottom of the loading block. As shown in **Figure 4**, each load gauge is made by attaching two steel plates whose face size is 10cm× 10cm and a steel pipe. We obtain the axial force acting on the plate, i.e. the contact force, with a set of the strain gauges on the pipe.

(2) Rubble rocks

The rubble rocks used in this test are the same ones used at actual construction sites in port areas of Japan. It is very important to use actual rubble rocks in this test since there have been no established similitude for load support systems of irregular-shaped particles as rubble rocks. Therefore, a small-scaled model test using smaller rocks and a corresponding loading plate, will not simulate the load support systems in-situ.

In this test, granite rubble rocks are used. The rocks have irregular shapes and wide size

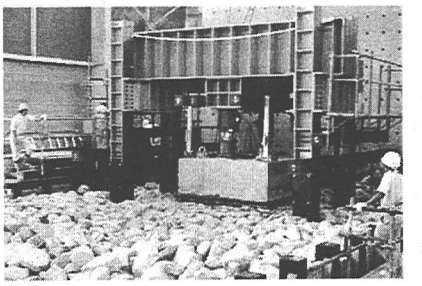

Fig.2 Loading test apparatus

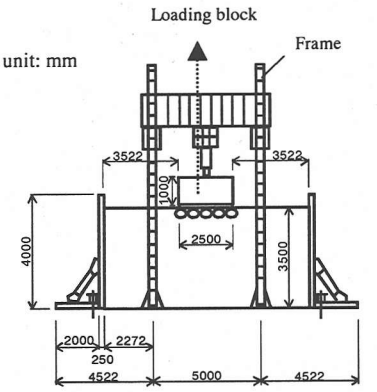

(a) Front view

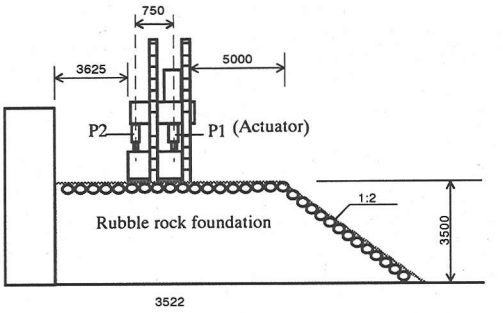

(b) Cross sectional view

Fig.3 Front and cross sectional views of loading test

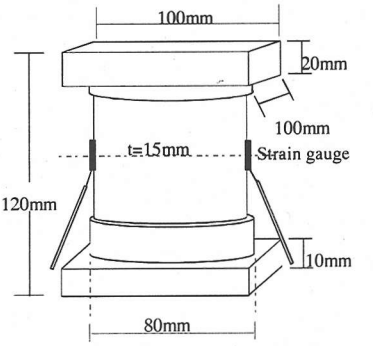

Fig.4 Load gauge

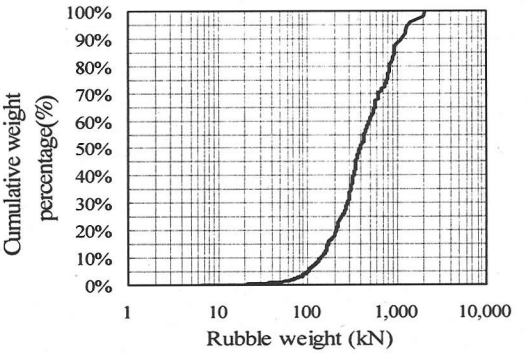

Fig.5 Weight distribution curve of ruble rock

Table 1 Loading test cases

CASE	Roughness (cm)	Thickness of foundation (m)	Standard deviation of foundation surface (cm)
CASE1	5	3.5	3.7
CASE2	30	3.5	5.1
CASE3	30	1.5	5.1
CASE4	30	3.5	5.1
CASE5	5	1.5	3.9
CASE6	30	1.5	4.9

Table 2 Loading conditions

Loading step	Loading condition	Actuator load (kN)		Average vertical stress (kPa)	Toe pressure (kPa)	
		P_1	P_2		q_1	q_2
1	Vertical	223	223	100	100	100
2		536	536	200	200	200
3	Inclined	862	834	300	309	290
4		1189	1133	400	419	381
5		1524	1422	500	534	466
6		1863	1708	600	652	548
7		2104	1906	670	737	604
8		2341	2107	740	819	662
9		2562	2260	800	902	699
10		2815	2444	870	994	745
11		3069	2629	940	1088	792
12		3286	2785	1000	1168	832
13*		4966	2855	1280	1989	571

*:cases 4 & 6

distributions since they are crushed rocks delivered from the nearest site. **Figure 5** shows weight distributions of the rubble rocks. The weight of the rubble rocks is between about 40 N and 2000 N. Though it is difficult to measure shapes and sizes of rubble rocks, the average length of the long axis of the rocks is about 30 cm while the largest and smallest lengths are about 80 cm and 10 cm respectively.

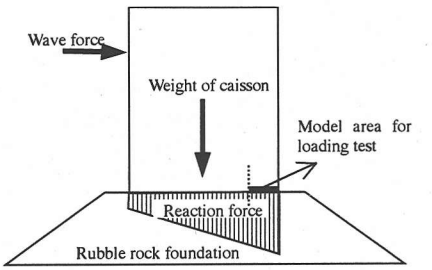

Fig.6 Schematic view of reaction force distributions on the bottom of a caisson due to wave force

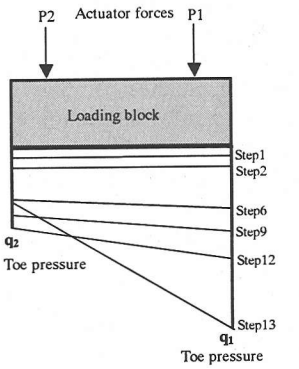

Fig.7 Reaction force distributions on the bottom of loading block at each loading step

(3) Test conditions

a) Test cases

In order to investigate the effects of the surface roughness and thickness of the foundation, we conducted six test cases as shown in **Table 1**. The Case1 and Case5 are for the smooth roughness foundations and the other cases are for the rough surface foundations. The planned height of the foundation is given as 3.5 m or 1.5 m. We conducted two test cases under the same test conditions for the rough surface foundations in order to confirm the reproducibility. This is because we thought that rougher surface foundations might give more random test results compared with those for the smoother surface foundations. Those are Cases 2 and 4 (R=30cm, H=3.5 m), and Cases 3 and 6 (R=30cm, H=1.5 m).

b) Loading conditions

After constructing the test foundation, we placed a loading block on the foundation. The block is then gradually loaded vertically by the two actuators located over the block. Initially, the foundation was loaded up to about 200 kPa (kN/m^2) of vertical stress on the bottom of the block. This stress level corresponds to the stresses in a caisson resting on a

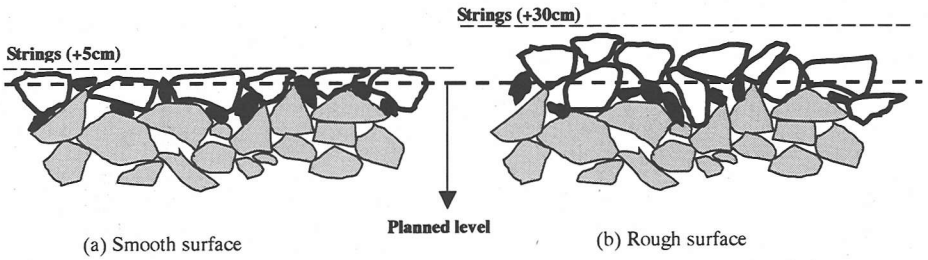

Fig.8 Schematic view of "Smooth surface" and "Rough surface" of a rubble rock foundation

rubble rock foundation at an actual site. Once the stress level is 200 kPa, the effects of horizontal wave forces as shown in **Figure 6**, acting on the foundation, are simulated by applying inclined load conditions. The test loading conditions are shown in the **Table 2** and reaction load distributions on the bottom of the block at each loading step are shown in **Figure 7**. It should be noted that these linear load distributions are calculated by assuming that the vertical loads generated by the actuators are linearly distributed between the foundation and the loading block. For this linear load distribution, vertical stresses at both edges and at the center are defined as "toe pressure" and "average vertical stress" respectively as shown in the **Table 2**. In this paper, we use this average vertical stress as a reference stress level on the foundation.

(4) Surface roughness of foundation

Here, we describe the construction procedure of the foundation surface based on our observations of the divers' working in the test and their subsequent explanations. Here we also clarify the differences between the smooth and rough surfaces from the point of view of the construction procedure.

a) Construction of surface roughness in-situ

In the construction of rubble rock foundations in-situ, the rubble rocks are first dropped into the sea from a ship until the height of the foundation is close to the planned level. After the settlement of the rubble rocks, the divers place a set of guide strings at the allowable height above the planned level of the foundation as shown in **Figure 8**. Normally, the divers place the guide strings at an interval of about 10 m or less in-situ. The divers then rearrange the rubble rocks to make the foundation surface flat with using the guide strings. According to the construction criteria for the surface roughness of a rubble rock foundation for port facilities in Japan[2], the smooth and rough surfaces are defined as the foundation surfaces whose heights are within ±5 cm and ±30 cm from the planned level respectively. The smooth surface is constructed in the areas where a caisson rests on, and the rough surface is constructed in the remaining areas of the foundation.

b) Construction of surface roughness in test

In order to reproduce a foundation surface at the actual construction sites, we hired three expert divers and asked them to construct the test foundation surfaces in the same manner as they do at the actual construction sites. Therefore, the construction procedure in this test is basically the same as that in-situ. In constructing the smooth surface in test, the guide strings were placed only at the surrounding boundaries of the projected area of the loading block. After the placement of the guide strings, the divers place relatively large rocks (indicated by white color in **Figure 8(a)**) on the top of the foundation not to exceed the string level. At the same time, the divers place the large rocks so that their flat surface face toward the bottom slab of a caisson. In addition to arranging the large rocks, the divers also use relatively small rocks (indicated by black color in the figure) to fill in the gaps between the large rocks so the large rocks cannot rotate or move. During the construction, the divers spent much time finding the best positions for the small rocks to insert into gaps, and determining the best combination of the small rocks and the large rocks so that the large rocks would be very stable. In the test, it took about 4 hours for three divers to construct the smooth surface area (2.5m×2.5m).

In the construction of the rough surface, the small rocks are not used to stabilize the large rocks. However, the divers still try to place the large rocks so that the surface is as flat as possible in the same manner as they did for the smooth surface. At this time, the divers pay less attention to the direction of the flat surfaces of the large rocks and their stability. Therefore, we say that the major part of the construction procedure conducted by the divers to produce for the smooth and the rough surfaces is identical. Futhermore, we note that the divers did

not need the guide strings 30cm above the planned level (**Figure 8(b)**) to construct the rough surface. Because of this simplified construction procedure, in this test, the construction time for the rough surface was reduced by about 50% compared with the smooth surface.

c) Characteristics of surface roughness in test

Before each loading test, we measured the foundation surface height by using a staff with a circular plate at its end whose diameter is 2.5 cm. We measured the foundation surface at 10 cm intervals and placed the staff at the projected position of each load gauge corner. Accordingly, the surface height was measured at 676 points for the area of the bottom of the loading block (2.5m×2.5m). **Figure 9** shows frequency distributions of measured heights from the planned level of the foundation surfaces ((a) smooth surface, (b) rough surface). From the figure, we note several characteristics of the foundation surface in the test.

Firstly, we see a similar shape of the height distribution for all the test cases if we shift each distribution to match each other in the figure. This is because, as described before, the divers construct the foundation in a similar manner regardless of the different surface roughness. This is especially true for the rough surface, as the divers could make a much rougher surface since the allowable range of the rough surface is ±30 cm, however, they did not do so.

Looking at the results further, we find that the smooth surface has a narrower distribution than the rough surface. This is because, as described before, the divers placed the large rocks so that their surface was flatter in the smooth surface. Evaluating this height difference with a standard deviation of the measured heights, we obtain about 3.8 cm and 5 cm standard deviations for the smooth and the rough surfaces respectively as shown in **Table 1**. This difference is not that large, however, we consider these smooth and rough surfaces in this test are representative surfaces at the actual construction sites since we explicitly asked the divers to construct the surfaces in the same manner as they do at the actual construction sites.

In addition, it should be noted that the smooth roughness has some larger and smaller heights beyond the allowable range for the smooth roughness, i.e. ±5 cm from the planned level. These smaller heights may exist because we used a smaller plate (diameter =2.5 cm) on the staff instead of a wider plate (diameter =7 cm) that is usually used in the actual surveys for the rubble rock foundations in-situ. In the test, we observed that the small plate

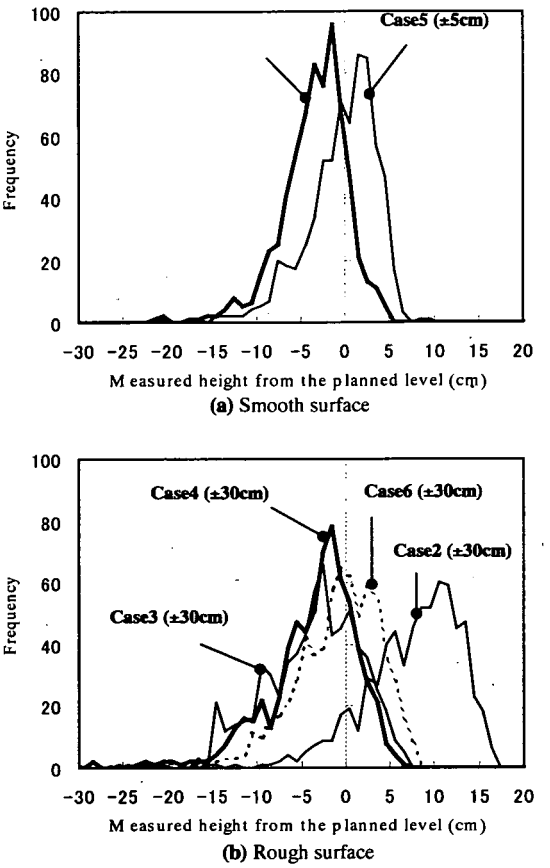

Fig.9 Frequency distributions of foundation surface height

was able to get into deeper gaps with small frontages between rubble rocks. This resulted in the wide height distributions in the left side.

The larger heights may also exist because of the following two reasons. Firstly, we should notice that the divers judge by their feel if the top level of a rubble rock exceeds the allowable height. Because the guide strings exist only at the boundaries of the surface construction area. This obscurity of the level judgment for a rubble rock may cause the larger heights beyond the allowable height in the test. In other words, the divers cannot control the surface differences observed in the smooth foundation cases (Cases 1 and 5). Secondly, we should notice that we assigned an extremely short interval of the height measurement for the test. In the test, an interval of 10 cm was used, whereas a 5 m interval is commonly used in the actual surveys for the foundations. Therefore, we consider that we were able to detect a much higher level of surface roughness in the foundation because of the precise height measurements performed in the test.

3. EXPERIMENTAL RESULTS

(1) Deformation of foundation

In order to illustrate general deformation characteristics of the test foundation due to the vertical loading and the effects of the surface roughness and the foundation thickness on the deformations, we here show **Figures 10** and **11**. These figures show the average settlement and the inclination of the loading block for all test cases with the increasing average vertical stress. The average settlement is defined at the center of the block and the inclination is defined as a clock-wise rotation angle of the loading block in the upper part of **Figure 10**. The reference settlement was defined at the moment when the bottom of the loading block touched the foundation. From the figure, we find that the surface roughness and the foundation thickness do not seem to affect the block deformations in this test.

However, in this figure, it can be seen that a larger height foundation (for example Case2, H=3.5 m) settled more than the smaller height foundations (for example Cases 3 and 6, H=1.5 m) even though all these foundations were assigned the same surface roughness. This unexpected result might be affected by the definition of the reference settlement in this test and also by a structure stability of the foundation near the surface. As shown before, the reference settlement was defined at the moment when the bottom of the loading block touched the foundation. Suppose, a single rubble rock is located on the foundation surface at the highest level. This means that the structure of this foundation surface is less unstable against the vertical loading effects. In this situation, the average settlement of the loading block will become larger within relatively lower stress levels.

This uncertainty of the structure stability of the foundation surface, which cannot be controlled even by expert divers, will be one of the reasons for the unexpected settlement results. This also affects the test reproducibility. You can also find that the average settlements measured under the same test condition, for example Cases 2 and 4, are quite different. Of course, this difference results from the in-homogeneity of the rubble rock foundations constructed in this test, in addition to the surface structure effects and the reference settlement definition. As shown above, it is very difficult to explain the settlement characteristics observed in this test, and we do not further describe this topic in this paper.

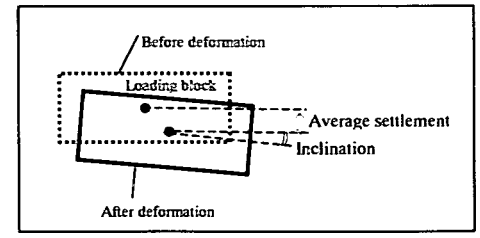

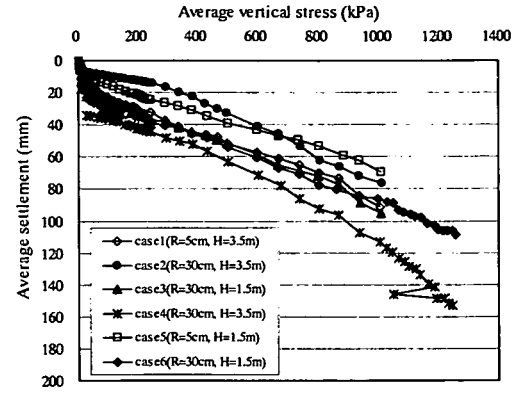

Fig.10 Settlement of loading block

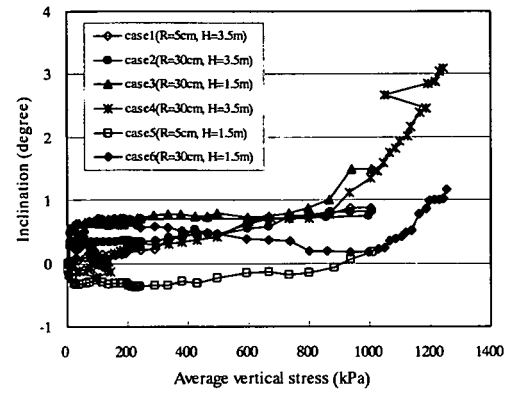

Fig.11 Inclination of loading block

(2) Characteristics of load support system

Figure 12 shows the contact force distributions between the rubble rocks and the loading block for the smooth surface case (Case1) when the average vertical stress is 200 kPa, 600 kPa and 1000 kPa. The three stresses correspond to the stress levels of the bottom slab of a caisson when the caisson is resting on a rubble rock foundation at the actual construction site (200 kPa), the caisson is loaded by maximum design wave force (600 kPa), and the caisson is loaded by an extreme wave force (1000 kPa). In the figures, individual contact force recorded by each load gauge is color coded according to the support percentage of the total load acting the bottom of the loading block. Shapes of

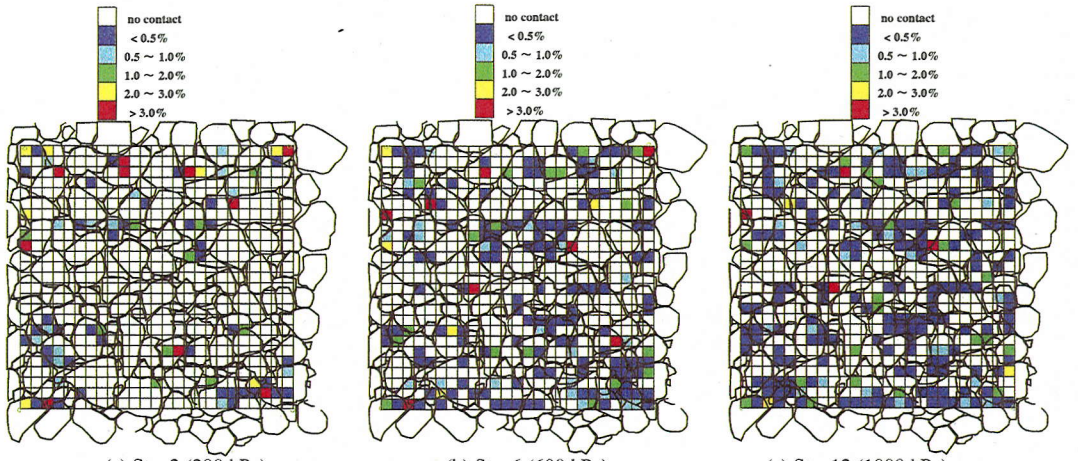

(a) Step2 (200 kPa) (b) Step6 (600 kPa) (c) Step12 (1000 kPa)

Fig.12 Contact force distributions between rubble rocks and loading block for smooth surface (Case1)

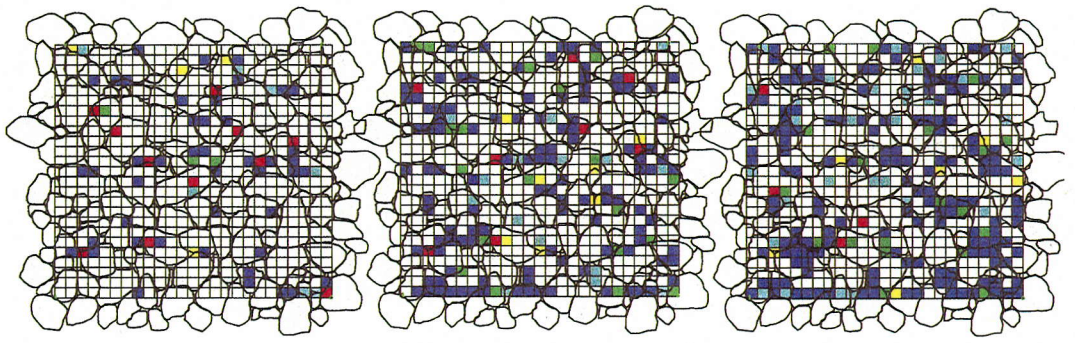

(a) Step2 (200 kPa) (b) Step6 (600 kPa) (c) Step12 (1000 kPa)

Fig.13 Contact force distributions between rubble rocks and loading block for rough surface (Case4)

the rubble rocks are also shown in the figures. As for the precision of the contact force measurement using the loading gauges, we believe that the measurement was very successful since the deviation of the total force measured by the loading gauges from that measured by actuators was within ±15 % in the most loading steps.

From the figures, we find that the loading block is supported by a small number of contact points even at the maximum stress level (1000 kPa). Looking at the three stress levels (200 kPa, 600 kPa and 1000 kPa), we find that the loading block has only 80, 176 and 212 contacting gauges out of the total gauges (625). Moreover, the vertical total load is not evenly distributed between contact points and the contact forces have a wide range of amplitudes even for the smooth surface foundation. For example, for the 200 kPa case (**Figure 12(a)**), we find that the large contact forces with red color support 51% of the total load with only 10 contact points. On the other hand, there are many small contact forces with dark blue color (38 contact points), however, they support only a small portion (6%) of the total load.

Figure 13 provides the same figure for the rough surface foundation (Case4). Comparing smooth and rough cases, we are able to conclude that the characteristics of the load support system seem almost the same in both cases. Note, in the rough surface case for 200 kPa, the large (red color) and the small (dark blue color) contact forces support 75% and 7% of the total load with 11 and 45 contact points respectively. Note, we also observed the same characteristics of load support system for the other test cases not reported here. Therefore, for a caisson resting on a rubble rock foundation, we conclude that it is supported by a discrete and inhomogeneous load support system regardless of the vertical stress level and the degree of the surface roughness. Furthermore, we have shown that this load support system differs significantly from linearly distributed load support system, which is assumed in the present design code.

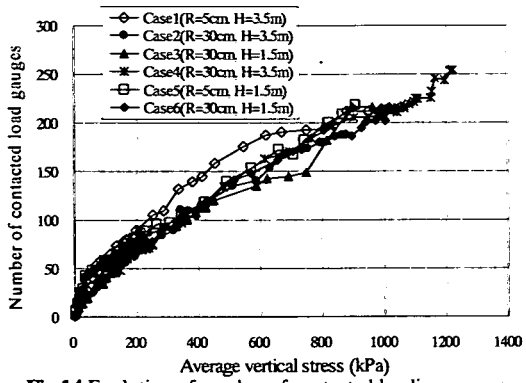

Fig.14 Evolution of number of contacted loading gauges

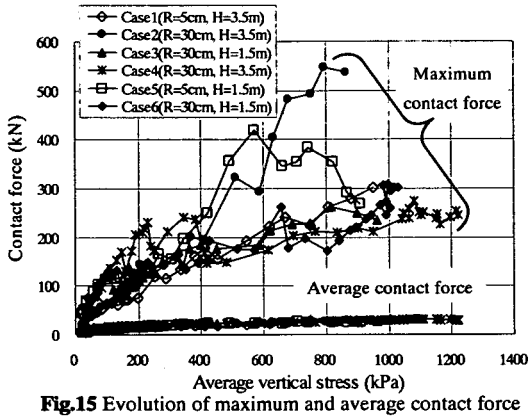

Fig.15 Evolution of maximum and average contact force

Figure 14 shows that the number of contact points remains the same at the same stress level for all test cases. **Figure 14** also shows that the evolution of the number of contacting gauges on the bottom of the loading block with the increasing vertical stress. The similarity in the evolution of the number of contacts in all six cases indicates that the load support system in these tests is not dependent on the surface roughness or the foundation thickness. Similarly from **Figure 15**, which shows the evolution of the maximum and average contact forces, we conclude that the maximum and average contact forces on the bottom of the block are not dependent on the surface roughness or the foundation thickness. Note, **Figures 14** and **15**, show that the number of contact points and the average contact forces are almost identical at the same stress level for all the cases. On the other hand, **Figure 15** indicates that the independency of the load support system with respect to foundation surface roughness and foundation thickness. This conclusion is based on the significant differences in the maximum contact force between the six test

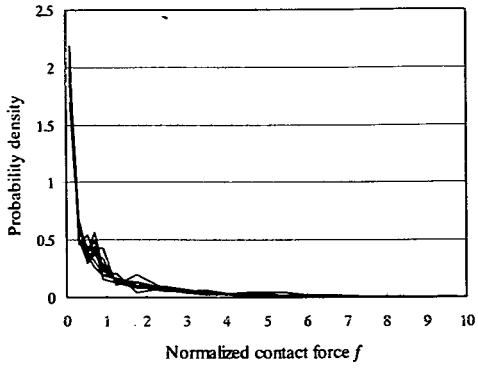

Fig.16 Probability distribution of normalized contact force (Case1: R=5cm, H=3.5m)

Table 3 Contact points percentage of normalized contact force

Normalized contact force	Case1 (R=5cm. H=3.5m)	Case2 (R=30cm. H=3.5m)	Case3 (R=30cm. H=1.5m)	Case4 (R=30cm. H=3.5m)	Case5 (R=5cm. H=1.5m)	Case6 (R=30cm. H=1.5m)	Average
0 - 1	70.5%	69.1%	69.2%	73.2%	71.2%	70.2%	70.6%
1 - 2	13.7%	15.3%	15.0%	10.5%	12.4%	14.3%	13.5%
2 - 3	7.2%	7.5%	6.7%	6.1%	7.3%	5.8%	6.8%
3 - 4	3.3%	3.4%	4.5%	3.4%	4.4%	3.4%	3.8%
4 - 5	2.1%	1.7%	1.7%	2.4%	2.5%	2.8%	2.2%
5 - 6	1.4%	1.5%	0.9%	1.7%	0.6%	1.8%	1.3%
6 - 7	0.8%	0.6%	0.7%	1.5%	0.2%	0.8%	0.8%
7 - 8	0.4%	0.4%	0.8%	0.5%	0.8%	0.5%	0.6%
8 - 9	0.4%	0.1%	0.4%	0.2%	0.1%	0.1%	0.2%
9 - 10	0.1%	0.2%	0.1%	0.0%	0.2%	0.2%	0.1%
10 - 20	0.3%	0.3%	0.0%	0.3%	0.4%	0.0%	0.2%
Total	100.0%	100.0%	100.0%	100.0%	100.0%	100.0%	100.0%

Table 4 Load support percentage of normalized contact force

Normalized contact force	Case1 (R=5cm. H=3.5m)	Case2 (R=30cm. H=3.5m)	Case3 (R=30cm. H=1.5m)	Case4 (R=30cm. H=3.5m)	Case5 (R=5cm. H=1.5m)	Case6 (R=30cm. H=1.5m)	Average
0 - 1	19.9%	18.2%	19.7%	18.1%	19.6%	19.4%	19.1%
1 - 2	19.7%	22.4%	21.7%	15.1%	18.1%	20.5%	19.6%
2 - 3	17.5%	18.3%	16.2%	15.1%	17.9%	14.3%	16.6%
3 - 4	11.3%	11.9%	15.6%	12.2%	15.1%	12.1%	13.0%
4 - 5	9.5%	7.5%	7.5%	11.1%	11.0%	12.6%	9.9%
5 - 6	7.5%	8.1%	5.0%	9.4%	3.1%	9.7%	7.1%
6 - 7	4.9%	3.9%	4.6%	9.7%	1.5%	4.9%	4.9%
7 - 8	3.0%	2.8%	5.9%	4.2%	5.9%	3.6%	4.2%
8 - 9	3.2%	0.5%	3.1%	2.0%	0.6%	0.9%	1.7%
9 - 10	0.8%	1.6%	0.8%	0.0%	1.4%	1.9%	1.1%
10 - 20	2.7%	4.7%	0.0%	3.1%	5.7%	0.0%	2.7%
Total	100.0%	100.0%	100.0%	100.0%	100.0%	100.0%	100.0%

cases. For example, at around 600 kPa of vertical stress, the largest and the second largest maximum contact forces are given in the smooth (Case5) and rough (Case2) surface foundations respectively. Before we performed the six tests, we assumed that the rougher surface would always generate a larger maximum contact force than the smooth surface however the test results have shown this is not true.

Finally, we investigate the internal structure of the load support system, i.e., contact force distributions. **Figure 16** shows the probability

distribution of normalized contact force amplitude f for all loading steps of Case1. The normalized contact force is defined by dividing individual contact force by the average contact force at each vertical stress level of each test case. The distributions indicate that there are many contact points that generate relatively small forces ($f<1.0$) while there are few contact points that produce relatively large forces ($f>1.0$). The large contact forces ($f>1.0$) form a long-tailed decay at the right side of the distribution. In this paper we do not further describe this decay in the normalized contact force distribution. However, note similar force distribution behavior has been reported elsewhere in the following studies. This research has shown an exponential decay at large contact forces ($f>1.0$) within an particulate assembly; for example: a) a series of uniaxial compression tests using glass bead packs by Mueth et. al[3], b) a theoretical model proposed by Lie et. al[4] and Coppersmith et. al[5], and c) numerical simulation results using the Discrete Element Method (DEM) by Radjai et. al[6] and Miyata et. al[7]. Therefore, this exponential decay seems to be a major characteristic of a contact force distribution within an assembly of particulate media such as rubble rocks.

More details on how the total load is supported by each class of the normalized contact force are given in **Tables 3** and **4**. The percentages of the contact points and load support ratio within each class of normalized contact force are reported in **Tables 3** and **4** respectively. These percentages for each test case are calculated by averaging the results at all stress levels shown in the **Table 1**. This can be done because the vertical stress level does not affect the percentages. From these results, we find that a small number of contact points (about 30%), that generate relatively large contact forces ($f>1.0$), support a large portion (about 80%) of the total load. Note, this phenomena is independent on the foundation surface and the foundation thickness. Therefore, we confirm again that this internal structure of load support system is not dependent on the surface roughness or the thickness of the foundation.

4. DESIGN CONSIDERATIONS

In this section, we focus our investigations on the effects of the inhomogeneous load support system on the bending moment amplitudes of the bottom slab of a caisson. Note the inhomogeneous load support systems obtained in these tests, are expected to increase the bending moments because of the concentrated load effects. On the other hand, the assumed linearly distributed load support system in the current design does not imply such a bending moment increase. In order to quantify the bending moment increase because of the inhomogeneous load support system, we conducted a series of FEM analyses of a square slab under both the experimental load condition and linearly distributed load condition at the same vertical stress level and compared the two results.

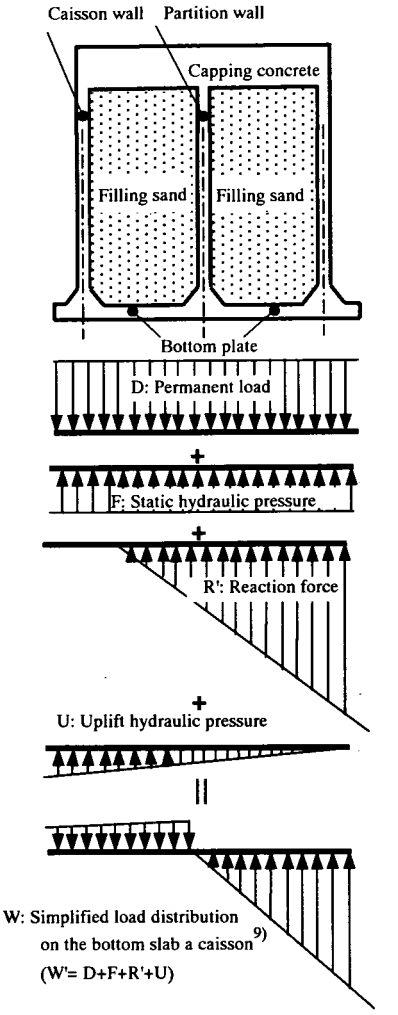

Fig.17 External forces acting on the bottom plate of a caisson in the current design

(1) Design method for the bottom slab of a caisson

In the design of the bottom slab of a caisson, the bending moments acting on the slab are calculated by considering several external forces as shown in

Table 5 FEM analysis parameters

Plate dimensions	plate size (X and Y)	2.5m x 2.5m
	thickness (Z)	0.6m
FEM model	element size (X and Y)	0.05m x 0.05m
	element thickness (Z)	0.06m
	boundary condition	all clumped
Material properties of plate	material	concrete
	Young's modulus	25 MN/m^2
	Poisson's ratio	0.167

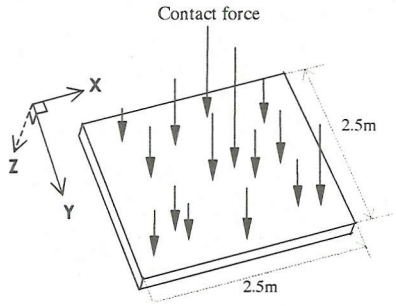

Fig.18 Schematic view of FEM model for a plate

Figure 17. These loads include: a) the dead weight of the filling sands, capping concrete and bottom slab (D: permanent load), b) the reaction force from the foundation due to the dead weight of a caisson and the horizontal wave force (R': reaction force), and c) the static and dynamic hydraulic pressures from the bottom of the slab (F: static hydraulic pressure, U: uplift hydraulic pressure). In the design, we assume that caisson walls and partition walls shown in the figure are rigid, and that the bottom slab is a rectangular slab whose surrounding boundaries are completely clamped to the caisson walls or the partition walls.

The design bending moments at a given location of a square slab under linearly distributed load conditions (M_{linear}) can be calculated using Levy's analytical solutions[8] with the following equation;

$$M_{linear} = CqL^2 \qquad (1)$$

where q is the vertical stress, L is the span of slab and C is a moment coefficient. In the design code[9], various moment coefficients are given in accordance with the geometry of the slab, loading conditions and boundary conditions.

(2) FEM analysis

Figure 18 shows a schematic view of the FEM analysis of the slab. We modeled a clamped-square slab whose planar dimensions are the same as the

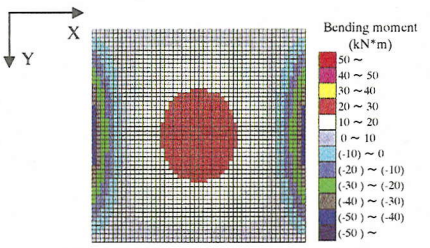

(a) Uniform distributed load condition

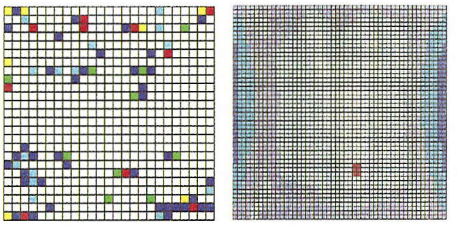

(b) Case1 (smooth surface)
(left: contact condition, right: bending moment)

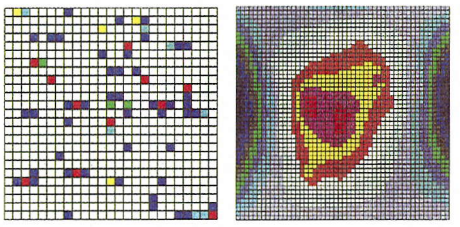

(c) Case4 (rough surface)
(left: contact condition, right: bending moment)

Fig.19 Bending moment distributions of a slab in the X direction at 200 (kPa) of vertical stress

bottom of the test loading block in order so we could apply the same contact forces in the FEM model at their locations, which were recorded during the test. Though the model span (2.5m) is much shorter than that used for a typical caisson in-situ (5m), in this study we do not consider the size difference effects. In the FEM model, the span is discretized into 50 elements so that the total number of elements in the model is 2500. Within the model slab, individual contact force is applied at the center of each corresponding load gauge location. Note, the thickness of the plate is 0.6m and discretized into 10 shell elements. **Table 5** shows parameters for the FEM analysis.

In this analysis, we simulated all the test loading steps shown in **Table 1**. We also simulated the slab subjected to a linearly distributed load in order to compare the bending moments generated by the experimental load conditions and the linearly distributed load conditions. Using the results from

these two different types of analyses, we were able to investigate the effects of the inhomogeneous load support system acting on the bottom slab of a caisson. These effects were quantified in terms of the bending moment amplitudes and spatial distributions. This information was then analyzed to determine the differences from bending moments developed from calculations based on the design assumptions.

(3) FEM results

Figure 19 shows the experimental contact conditions and bending moment distributions in the X direction at 200 kPa : (a) uniformly distributed load condition, (b) Case1 (smooth surface) load condition, and (c) Case4 (rough surface) load condition. From the figures, we note two important points.

Firstly, the locations of contact points which have large contact forces, strongly affect the spatial distributions of the bending moment on the slab. Under a uniformly distributed load condition, the positive maximum moment is generated exactly at the center of the slab. However, the location of the positive maximum bending moment varies and is strongly dependent on the locations of the large contact forces when the slab is subject to an experimental load condition. Similar behavior is also noted for the negative maximum bending moment on the surrounding boundaries. The effects of the large contact forces on the spatial distributions of the negative bending moment seem to be relatively small compared with the effects on the positive maximum bending moment at the center.

Secondly, the bending moments generated by the experimental load conditions are likely to differ significantly from the design bending moments. For example, the bending moments developed in Case1 (smooth surface) are smaller than the design moments, whereas the moments developed in Case4 (rough surface) are greater than the design moments. Later in this section, we describe the reason for this behavior. We also show that such an increase or decrease of bending moment is more dependent on the locations of the large contact forces rather than the degree of the surface roughness.

Here, we investigate the factors that increase or decrease the bending moment. **Figure 20** shows the ratio of positive maximum bending moments generated around the center of the slab. This ratio is calculated by dividing the maximum bending moment generated under the experimental load conditions by that generated under the linearly distributed load condition. From the figure, we find

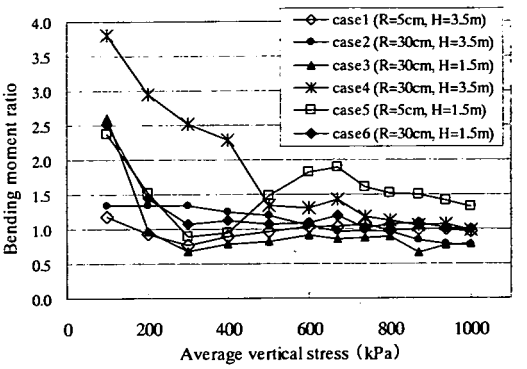

Fig.20 Positive maximum bending moment ratios around the center of slab (Experimental / Uniform load conditions)

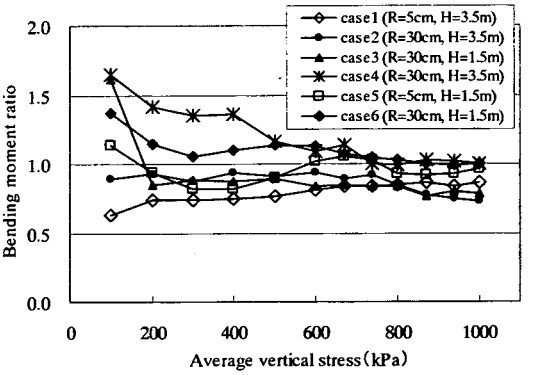

Fig.21 Negative maximum bending moment ratios on the edge of slab (Experimental / Uniform load conditions)

that maximum bending moments near the center in several cases become quite large because of the inhomogeneous load support systems, especially at the low stress level (less than 200 kPa). This moment increase is gradually alleviated with an increase of the vertical stress. This is because the number of contact points increases with the vertical stress and the concentrated load effects are gradually reduced. However, looking at the higher stress levels around 500 kPa which are similar to the design conditions for a caisson slab, the moment ratios in some test cases are still greater than unity. Moreover, note the maximum ratio among the test cases is given by the smooth surface case (Case5). This result indicates that it can be important to consider bending moment increases for the smooth foundations, at high stress levels over 500 kPa. Later in this section, we describe whether these moment increases are critically dangerous or not.

Figure 21 shows a similar plot for the negative maximum bending moment ratios at the edge. Note, this figure plots the largest of the bending moment ratios at the four edges of the slab. From the figure,

we find the same tendency as seen at the center moment ratios, however, the maximum moment ratios for the edge are much smaller than those predicted at the center. This is because the sensitivity of the concentrated loading near the center and near the edge with respect to the maximum bending moments are different. This behavior is described in the next section.

(4) Effects of locations of concentrated loading

In this section, we discuss the above-described sensitivity of the concentrated loading and clarify why the bending moments generated by the experimental load conditions are sometimes greater and sometimes smaller than the design bending moments.

Figure 22 shows a chart for calculating the positive and negative bending moments of a square clamped slab due to a single concentrated load. The location of the concentrated load is on the center line and is at a distance a from the edge. Using the moment coefficient (α) shown in this chart, we calculate the maximum bending moment (M_{point}) due to a concentrated (point) load by the equation;

$$M_{point} = \alpha P \qquad (2)$$

where P is the concentrated load. Note, the moment coefficient α is assigned a negative sign for the calculation of the negative maximum bending moment generated at the edge. In this case, the positive and negative maximum moments are always generated at the concentrated load point, and at the middle of the span at the edge that is closer to the load point, respectively. Note, this chart was obtained by a series of FEM analysis with varying locations of the concentrated load[10].

If we consider a condition where the maximum bending moments due to the linearly distributed load and the concentrated load are identical, we obtain the following equation using equations (1) and (2):

$$P = \left(C/\alpha\right) \times (q \cdot L^2) \qquad (3)$$

In this equation, the concentrated load P is the contact force intensity that generates the same maximum bending moment generated by a uniformly distributed vertical stress q. In this case, the minimum ratio (C/α) for the positive maximum bending moment at the center of slab is about 1/10 since C is 0.0206 and the maximum α is 0.205 respectively. Note, the moment coefficient C is given from the table included in the design code[9]

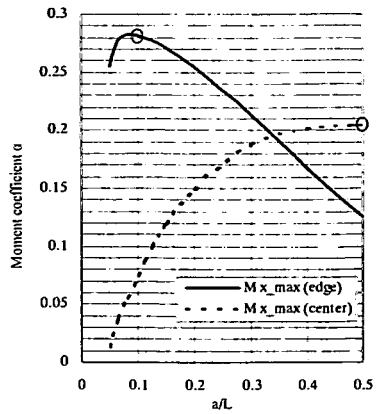

Fig.22 Chart of moment coefficient α for concentrated load[10]

and the coefficient α is obtained from **Fig.22** (a=0.5, Mx_max(center)). Therefore, the design maximum bending moment at the center (M_{linear}) can be generated by a single concentrated load whose amplitude is about 1/10 of the total load acting on the slab. Similarly, the design maximum moment at the edge (M_{linear}) can be generated by a single concentrated load which is about 1/5.5 of the total load, that is located at the 1/10 of the span length from the edge (C= −0.0513, α= −0.282). Note, the moment coefficient C is given from the table included in the design code[9] and the coefficient α is obtained from **Fig.22** (a=0.1, Mx_max(edge)). This directly shows that the maximum bending moment near the center is more likely to exceed the design maximum bending moment for smaller contact forces than the maximum bending moment at edges. This results in generating a larger moment ratio at the center (**Figure 20**) than the moment ratio at the edges (**Figure 21**).

The larger bending moment around the center of the slab is clearly shown in Case4. Looking at Case4 result at 200 kPa in **Figure 19(c)**, we find that some large contact forces are located near the center of the slab and that the slab has quite a large bending moment ratios, see **Figure 20**. This concentration of large contact forces around the center generates a large bending moment around the center of the slab. On the other hand, in Case1, the bending moment ratios are much smaller than the design bending moment as shown in **Figure 19(b)**. Note, this happens when many large contact forces are located extremely close to the edges (less than 0.05 of the span length) or near the corners of the slab. These results show that the location of large contact forces is the most important factor, which affects the

amplitudes and the spatial distributions of the slab bending moments.

5. CONCLUSIONS

(1) In this study, we conducted a series of vertical loading tests of a rubble rock foundation and succeeded in recording contact forces between rubble rocks and a loading block. The test results showed the following points:

a) The "smooth surface" and "rough surface" rubble rock foundations made by expert divers seem to be constructed in a similar manner. However, we noticed several minor differences. In preparation of the smooth surface, large rocks are placed on the surface so that their flat surfaces face against the bottom slab of a caisson. Additionally, small rocks are used to fill in the gaps so that the large rocks do not rotate or move. On the other hand, when the divers prepare a rough surface they still place the large rocks in the same manner as they do for the smooth surface. However, the divers pay less attention to the direction of the flat faces of the large rocks when making a rough surface. Moreover, the small rocks are not used to stabilize the large rocks for the rough surface.
b) The loading block on the smooth and rough foundations is supported by a small number of contact points and the contact force amplitudes have a wide range of distribution. This discrete and inhomogeneous load support system of the foundation is very different from linearly distributed load support system that is assumed in the present design for the bottom slab of a caisson.
c) The test results do not show a dependence of the load support system on the surface roughness or the thickness of the foundation. Since there is no significant difference in the load support systems between a "smooth surface" and a "rough surface" foundations constructed by expert divers, we are most likely to employ a "rough surface" instead of a "smooth surface" for rubble rock foundations at the actual construction sites, when the rubble foundations are constructed by expert divers.

(2) In order to investigate the effects of the difference of load support systems of a rubble rock foundation, i.e., inhomogeneous and homogenous support systems, on the amplitudes and the spatial distributions of bending moment of the bottom slab of a caisson, we conducted a series of FEM analyses where the slab size and loading conditions are the same in the test. From the results, we made the following conclusions:

a) Spatial distributions and amplitudes of positive /negative maximum bending moments on a square clamped slab, that are generated at the center and at the edges of the slab respectively, are strongly affected by the locations of contact points that have large contact forces.
b) Because of the discrete and inhomogeneous load support system of a rubble rock foundation, the maximum bending moments of the slab are likely to exceed the maximum design moments predicted by linearly distributed load support system. This tendency is noticeable at the low vertical stress level (less than 200 kPa) and for the positive maximum bending moment generated near the center of the slab. This tendency is gradually alleviated as the vertical stress increases because of the increase of the number of contact points on the slab.
c) Very large bending moments are more likely to occur near the center of the slab rather than at the edges. This is because the sensitivity of the concentrated loads near the center and near the edge of a square clamped slab with respect to the maximum bending moments are different. In other words, the maximum bending moments near the center of the bottom slab of a caisson are more likely to exceed the design maximum moment for smaller contact forces than the maximum bending moments developed at the edges of the slab.

Before concluding this paper, we briefly discuss the safety level of the bottom slab of caisson type breakwaters in-situ and our current work for the development of a new design method for the bottom slab.

Practically speaking, the current safety level of the bottom slab of a caisson type breakwater is considered quite high and the bottom slab is hardly damaged since there have been no damage reports of breakage or failure of the bottom slab of a caisson in-situ, as far as the authors know. Though there will be many reasons for this high safety level of the bottom slab, we consider the most possible reason is that internal safety level of structural members including the bottom slab is much higher than external safety level against sliding, turnover and foundation failure of breakwaters. In other words, a caisson type breakwater moves (sliding, turnover or foundation failure) due to external loadings before the bottom slab of the caisson is damaged. This evaluation is based on the results of reliability-based investigations by one of the authors[11]. We will further investigate safety margins in the current

design method and determine target safety level considering synthetic failure probability.

In addition to investigating the safety margins, we are now developing a new design method for the bottom slab of a caisson, which is capable of considering surface roughness effects on the bending moment increase or decrease. For that purpose, we are proposing to introduce new safety factors[12], which represent the surface roughness effects on the slab bending moment, into the current design method (Limit State Design Method). At the first stage, we are now trying to determine values of the safety factors by code calibration so that the safety level of the bottom slab under any different surface roughness conditions could be the same as the present safety level of the bottom slab under smooth surface condition created by expert divers. The new design method will be shown in our next paper.

ACKNOWLEDGMENT: The authors acknowledge financial and technical support from the Kanto Regional Construction Bureau of Ministry of Land, Infrastructure and Transport in Japan, including Mr. K. Shinohara, Mr. Y. Sano and Mr. T. Kondo. The authors also acknowledge Dr. H. Mizuno and Dr. H. Kato of Building Research Institute for their kindly lending recording systems for our experiment. The first author acknowledges all the members of Particulate Science and Technology Group (PSTG) at Colorado School of Mines, Dr. H. Tanaka of the Penta-Ocean Construction Co. Ltd., and Mr. Y. Shimizu of Penta-Techno Service Co. Ltd. for their helpful advise and comments. The authors also acknowledge that the loading test was conducted at the Technical Research Institute of Toyo Construction Co. Ltd. The loading gauges used in the test were made by Kyowa Electronic Instruments Co. Ltd., and the figures in the paper were prepared with great care and skill by Ms. M. Kobayashi.

REFERENCES

1) Miyata, M., Sugano, T., Nagao, T., Shinohara, K. and Kondoh, T.: The Effect of Surface Configuration of Rubble Mounds on the Stress on the Bottom Slab of Caisson, *Technical Note of the Port and Harbour Research Institute (PHRI)*, No.945, 1999. (in Japanese)

2) *Specifications for Port Constructions in Japan*, Bureau of Ports and Habours and Port and Harbour Research Institute, Ministry of Transport ed., The Japan Port and Harbour Association press, Tokyo, 1999. (in Japanese)

3) Mueth, D.M., Jaeger, H.M. and Nagel, S.R.: Force Distribution in a Granular Medium, *Physical Review E* 57, pp.3164-3169, 1998.

4) Liu, C.-h., Nagel, S.R., Shecter, D. and Coppersmith S.: Force Fluctuations in Bead Packs, *Science* 269, pp.513-515, 1995.

5) Coppersmith, S.N., Liu, C.-h. Majumdar S., Narayan, O. and Witten T.A.: Model of Force Fluctuations in Bead Packs, *Physical Review E* 53, pp.4673-4685, 1996.

6) Radjia, F., Jean, M., Moreau, J-J. and Roux, S., N. Force Distributions in Dense Two-Dimensinal Granular Systems, *Physical Review Let.* 77, pp.274-277, 1996.

7) Miyata, M., Mustoe, G.. G..W., Nakagawa, M., Sugano, T. and Tanaka, T.: Study on the Force Support System within a Rubble Rock Foundation using Discrete Element Method, *Powders & Grains 2001*, Balkema, Rotterdam, pp.267-270, 2001.

8) Ugural, A.C.: *Stresses in Plates and Shells*, 2nd ed., McGraw-Hill, New York, 1999.

9) *Technical Standards and Commentaries for Port and Harbour Facilities in Japan*, Bureau of Ports and Habours and Port and Harbour Research Institute, Ministry of Transport ed., The Overseas Coastal Area Development Institute (OCDI) press, Tokyo, 2002.

10) Sotozono, T.: Design Method for the Slab of Warehouse Facilities, *The Kenchiku Gijutsu*, No.536, pp.128-133, 1994. (in Japanese)

11) Nagao, T.: Reliability Based Design Method for Flexural Design of Caisson Type Breakwaters, *J. of Structural Mech. And Earthquake Eng.*, JSCE, No.696, I-58, pp.173-184, 2002. (in Japanese)

12) Miyata, M., Sugano, T., Nagao, T. and Kikuchi, N.: A New Design Method for Caisson Bottom Slab Considering Force Support Mechanism of a Rubble Rock Foundation, *Tsuchi-to-Kiso (The Japanese Geotechnical Society)*, Vol.50, No.4, Ser. No.531, pp.19-21, 2002. (in Japanese)

(Received April 9, 2002)